2008

Understanding Bake-Hardening in Modern High Strength Steels for the Automotive Industry Using Advanced Analytical Techniques

I. B. Timoknina
Monash University

P. D. Hodgson
Deakin University

S. P. Ringer
University of Sydney

R. K. Zheng
University of Sydney

E V. Pereloma
University of Wollongong, elenap@uow.edu.au

UNDERSTANDING BAKE-HARDENING IN MODERN HIGH STRENGTH STEELS FOR THE AUTOMOTIVE INDUSTRY USING ADVANCED ANALYTICAL TECHNIQUES

I.B. Timokhina[1], P.D. Hodgson[2], S.P. Ringer[3] R.K. Zheng[3] and E.V. Pereloma[4]

[1]Department of Materials Engineering, Monash University, VIC 3800, Australia
[2]Centre for Material and Fibre Innovation, Deakin University, Geelong, Vic 3217, Australia
[3]Australia Key Centre for Microscopy and Microanalysis, University of Sydney, NSW 2006, Australia

[4] School of Mechanical, Material and Mechatronics Engineering, The University of Wollongong, Wollongong, NSW 2522, Australia

Keywords: TRIP and DP steels, bake-hardening, Atom Probe Tomography, TEM.

Abstract
The bake-hardening behaviour of intercritically annealed, dual-phase (DP) and transformation induced plasticity (TRIP) steels was studied using X-ray diffraction, transmission electron microscopy (TEM) and three-dimensional atom probe tomography (APT). The DP steel showed an increase in the yield strength and the appearance of the upper and lower yield points after a single bake-hardening treatment compared with the as-received condition, while the mechanical properties of the TRIP steel remained unchanged. This appears to be due to the formation of plastic deformation zones with high dislocation density around the "as-quenched" martensite and segregation of carbon along these dislocations in the DP steel. Moreover, APT showed that the carbon content of polygonal ferrite in the DP steel was higher than in the TRIP steel. The carbon atom map of the DP steel after bake-hardening treatment also revealed the formation of Fe_3C carbides within the martensite crystal. APT of the TRIP steel showed the segregation of carbon around the dislocations in the retained austenite crystals.

Introduction
A major strategy to achieve the optimum combination of properties, cost and productivity is through the reduction of the vehicle weight by using a stronger material. Past efforts to the improve strength have concentrated on grain refinement, solid solution and precipitation strengthening. In most cases, an increase in strength is accompanied by a reduction in ductility. The search for new strengthening mechanisms, while maintaining adequate ductility, has led to the development of new multiphase steels such as dual phase (DP) steels and Transformation Induced Plasticity (TRIP) steels [1,2]. In these new steels, the complex microstructure can introduce defects, encourage transformation during deformation, or increase the work hardening rate in other ways [2].
The microstructure of DP steels consists of a soft, ductile polygonal ferrite matrix with hard martensite islands, and, in some cases, a small amount of retained austenite [3]. The strength-ductility balance in this steel is controlled by the volume fraction of martensite [3]. The TRIP steel microstructure contains polygonal ferrite, bainite, retained austenite and a minor quantity of martensite [4]. Both steels exhibit continuous yielding behavior, a low yield point and a high strain-hardening coefficient [5,6]. This has been attributed to an increase in work-hardening, through the continuous transformation of retained austenite to martensite in the TRIP steels and the formation of mobile dislocations and martensite twinning in the DP steels, during forming [7]. This results in a localized increase of the strain-hardening coefficient, which delays the onset of necking and ultimately leads to high elongation without compromising the strength [2].
In industrial processing these steels undergo a finishing treatment, where the paint coating of the automotive body is baked at temperatures of 150-200^{o}C for 20-30 min after forming [8]. During this

bake-hardening (BH) treatment, interstitial solute atoms, such as carbon, move to the dislocations produced during pressing and pin them [9]. The driving force for this solute redistribution is to reduce the lattice energy. This leads to the solute diffusion toward dislocations and the formation of a Cottrell atmosphere [10].
It has recently been proposed to use the BH treatment for both TRIP and DP steels to increase the yield strength of these steels in the final body structure [8]. This should potentially lead to an increase in strength for the same thickness of steel sheet. The yield strength increase was accompanied by the return of the yield point, a slight increase in the tensile strength and a decrease in the elongation [9]. Since there is no additional process step required, BH could result in good shape fixability and improved dent and crash resistance without affecting the production cost [8].
Although, the bake-hardening effect after pre-straining in the DP and TRIP steels has been intensively studied using X-ray analysis and transmission electron microscopy [11,12], the contribution of bake-hardening to an increase in yield strength has not been properly identified. It is important since bake-hardening response in these steels depends not only on the amount of pre-strain, bake-hardening temperature and time but also on the formation of mobile dislocations in ferrite as a result of martensite transformation during processing and contribution of these dislocation pinning to an increase in bake-hardening response is essential. Moreover, X-ray and TEM techniques are not able to provide accurate local analysis of the phases or a quantitative analysis of segregation to specific microstructure features, such as dislocations. In contrast, Atom Probe Tomography (APT) has the high spatial resolution required to provide accurate determination of the solute content in ferrite, martensite, retained austenite and bainite and measure the local composition of nanosized microstructural features such as solute clusters and segregations at dislocations.

The aim of the current study is to identify the effect of bake-hardening on microstructural features formed in the DP and TRIP steels after processing without taking into account the effect of pre-straining using advanced analytical techniques such as TEM and APT.

Experimental

The TRIP and DP steels used in the current work were produced by a standard cold rolling and intercritical annealing (IA) with the compositions shown in Table 1. To study the effect of the bake-hardening treatment on the mechanical properties, the samples were bake-hardened at 175^{o}C for 30 min.

Table 1. Chemical Composition of Steels.

Steel		**C**	**Si**	**Mn**	**Al**	**Cu**	**Cr**	**P**
TRIP	wt%	0.12	1.77	1.39	0.031	0.005	0.02	0.004
	at%	0.55	3.44	1.38	0.062	0.004	0.02	0.007
DP	wt%	0.036	1.065	1.08	0.018	0.004	0.083	
	at%	0.17	2.09	1.08	0.037	0.0035	0.088	0.01

Room temperature mechanical properties of the samples were determined using an Instron 4500 servohydraulic tensile testing machine with a 100kN load cell.
The microstructures of both steels were characterised using transmission electron microscopy (TEM). TEM analysis was carried out using a Philips CM 20, operated at 200kV. Thin foils for TEM were prepared by twin jet electropolishing using a solution of 5% perchloric acid in methanol at –20^{o}C and an operating voltage of 30V. Particle analysis of TRIP steel was carried out using the carbon extraction replica technique. Carbon replicas were prepared from 2% Nital etched samples that were carbon coated and then etched in 10% Nital to remove the carbon film. This film was then floated off in ethanol and collected on a Ni or Cu grid.
The dislocation density was calculated by measuring the total dislocation line length in a unit volume of crystal giving a parameter in terms of length (m)/m^3. Using this method, the dislocation density (Λ), is given by [13]:

$$\Lambda = 2N_L/Lt, \qquad (1),$$

where N_L is the number of intersections with dislocations, L is random line length and t is the foil thickness.
X-ray diffraction was carried out using a Philips PW 1130 (40kV, 25mA) diffractometer to identify the volume fraction and carbon content of retained austenite in the TRIP steel [14].
Atom Probe Tomography (APT) analysis was carried out using the local electrode atom probe (LEAP) at the University of Sydney's Electron Microscopy Unit. The standard two-stage electropolishing procedure was used to prepare atom probe specimens [15]. The local electrode atom probe was operated at a pulse repetition rate of 200 kHz, a 0.2 pulse fraction and with a sample temperature of 80K.

Results

Mechanical properties after processing and bake-hardening treatment

Both steels demonstrated a good combination of mechanical properties and continuous yielding behavior in as-received condition (Figs. 1a, b). The bake-hardening treatment caused the appearance of upper and lower yield points on the stress-strain curve of the DP steel, while the stress-strain behavior of the TRIP steel was continuous (Figs. 1 a, b). Moreover, the yield strength in the DP steel after BH increased ~ 150MPa over the as received condition, while the yield strength values for the TRIP steel were similar before and after heat-treatment (Figs. 1a, b). The total elongation values for both steels showed a slight increase (Figs. 1a, b). The strain-hardening rate curves after processing showed a continuous exponential decrease for both steels (Figs. 1c, d). The DP steel after bake-hardening treatment had a sharp rate of change, with evidence of a discontinuity (eg. local minima), while the strain hardening rate curve for the TRIP steel still showed a smooth, continuous decrease (Figs. 1c, d).

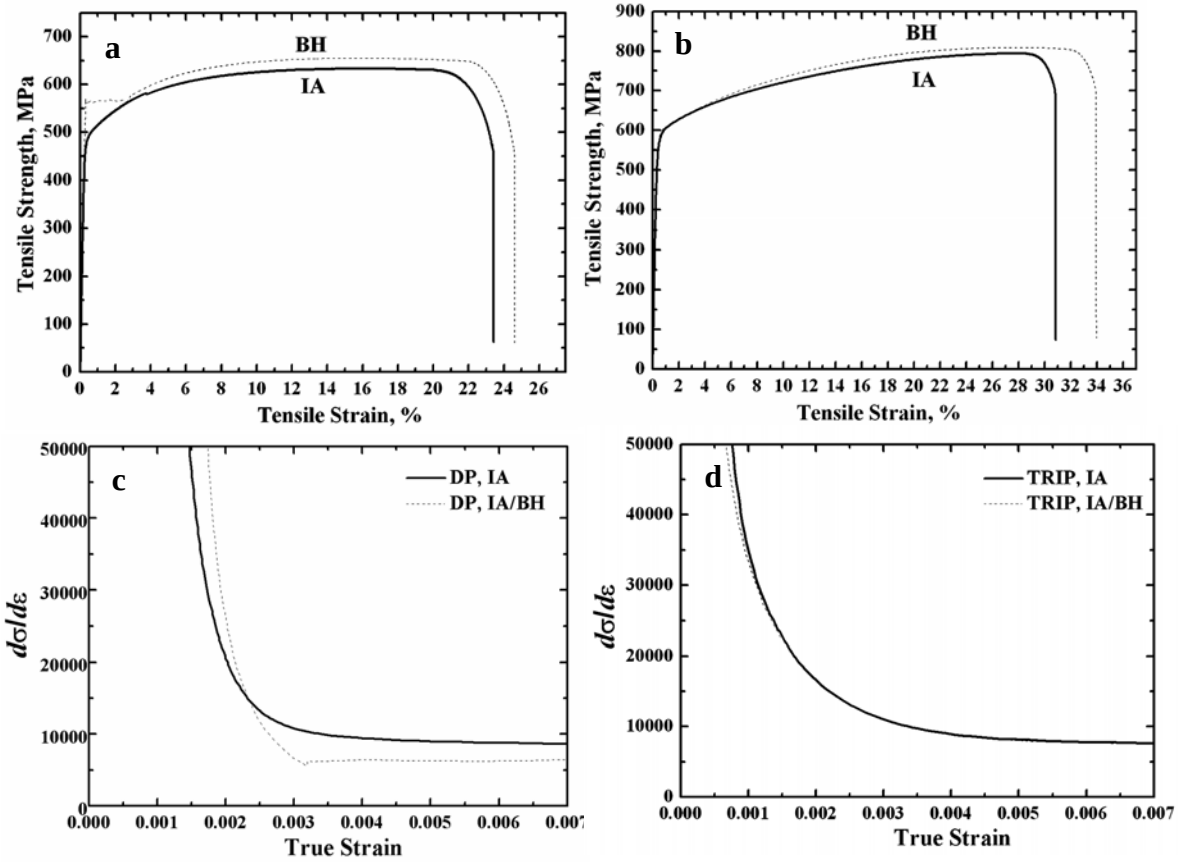

Fig. 1. Representative stress-strain curves (a, b) and variation of strain-hardening rate with true strain (c, d) of the DP (a, c) and TRIP steels (b, d).

TEM characterisation after processing and bake-hardening

The microstructure of the DP steel consisted of ~ 75±5% polygonal ferrite with a grain size of ~ 9±1.9μm and ~ 15±4% martensite (Fig. 2a). TEM also revealed the presence of a small amount of bainite and retained austenite. The dislocation density of polygonal ferrite in the DP steel was lower than the TRIP steel (Table 2). Despite this fact, the polygonal ferrite areas in the vicinity of martensite displayed an increase in the dislocation density to 5±0.8 $x10^{14}m^{-2}$ (Table 2) caused by the stress propagation of the martensite into the soft ferrite matrix associated with the volume increase when martensite forms (Fig. 2b). The microstructure of the DP steel was also characterized by a large number of fine and coarse Fe_3C carbides in the ferrite matrix and along single dislocations or on the dislocation pile-up in the ferrite matrix (Fig. 2c).

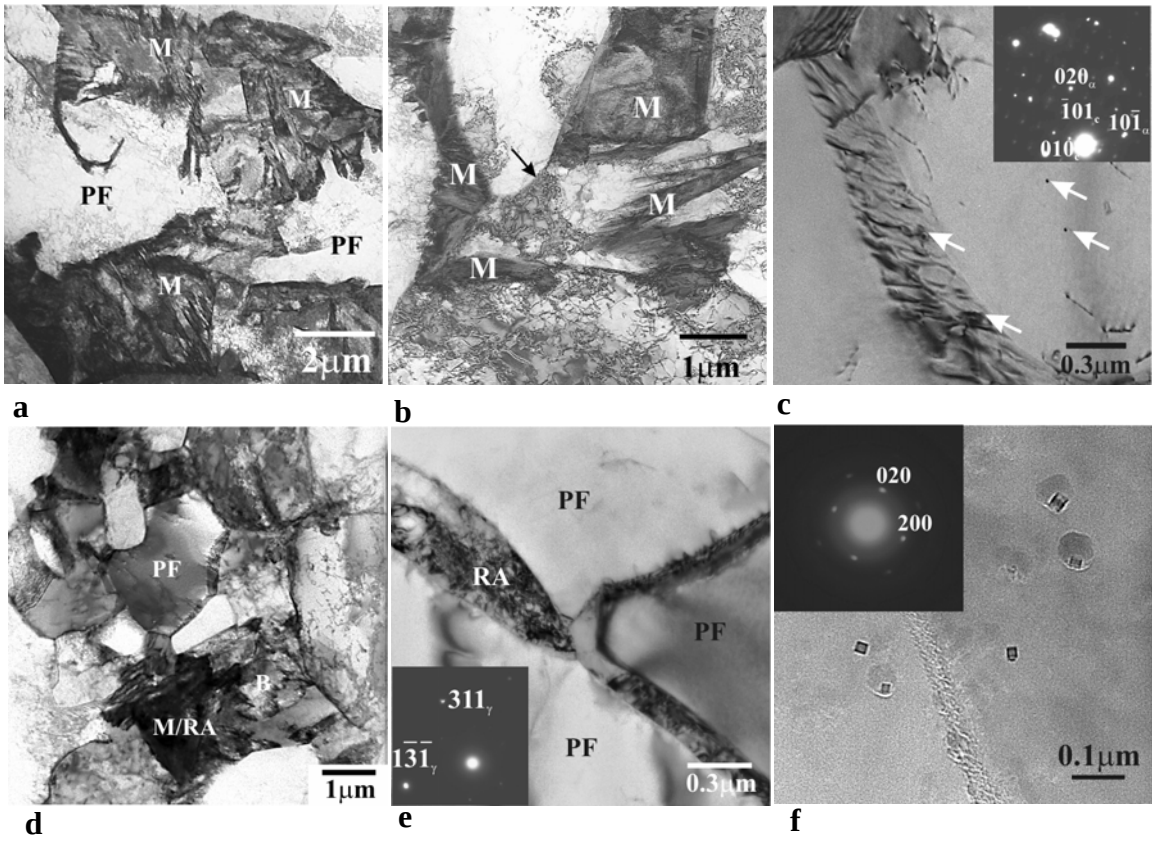

Fig. 2. TEM micrographs of studied steels after intercritical annealing: (a) DP steel microstructure after intercritical annealing, (b) formation of mobile dislocations at the martensite/ferrite interface indicated by arrows in the DP steel, (c) Fe_3C carbides (indicated by arrows) in the ferrite of DP steel ($[101]_\alpha//[101]_c$), (d) representative TRIP steel microstructure after intercritical annealing, (e) retained austenite in ferrite of TRIP steel (zone axis is $[12\bar{5}]_\gamma$) and (f) TiC carbides in the TRIP steel (zone axis is [001]). PF is polygonal ferrite, M is martensite, RA is retained austenite.

Table 2. Microstructural characterization of the dislocation structure in polygonal ferrite.

	DP		**TRIP**
	average	ferrite/martensite interface	average
Dislocation Density, $x10^{14}m^{-2}$	0.96±0.04	5±0.8	1.75±0.09
Average Distance between dislocations, nm	309±28	200±20	189±20

The microstructure of the TRIP steel was ~ 70±3% polygonal ferrite and ~20±3% retained austenite with an average carbon content of 5±0.02at%. The other main phases in the microstructure were bainite and martensite (Fig. 2d). The polygonal ferrite of the TRIP steel had a higher dislocation density than ferrite in the DP (Table 2) and a grain size of 4±1.5μm. The retained austenite appeared to be in the form of a martensite/retained austenite constituent between the bainitic ferrite, or as islands between the polygonal ferrite grains (Fig. 2 e). Carbon replica technique revealed the formation of TiC in the microstructure of the TRIP steel (Fig. 2 f) with a cubic lattice structure and a lattice parameter of *a*=0.424nm.

The TEM study of the DP steel after bake-hardening treatment revealed an increase in number of Fe_3C carbides in the polygonal ferrite and formation of fine Fe_3C carbides in martensite (Figs. 3 a, b). The X-ray study of the TRIP steel after bake-hardening treatment showed a slight decrease in the volume fraction of retained austenite. TEM microanalysis on the bake-hardened TRIP samples did not reveal significant microstructural changes compared to the as-received condition.

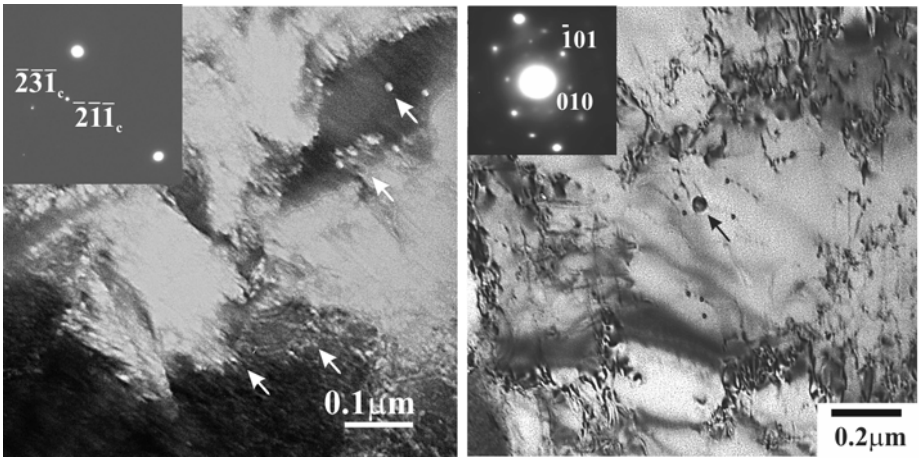

Fig. 3. TEM dark field image of Fe_3C carbides (zone axis is $[10\bar{2}]$) in martensite (a) and bright field image of Fe_3C in ferrite (zone axis is [101]) of DP steel after bake-hardening treatment.

APT characterisation of steels after processing and bake-hardening treatment

The APT study of the DP steel revealed the presence of two main regions: (i) carbon-depleted region with an average carbon content of 0.06±0.003at% and an Si average content of 2.3±0.02at% and (ii) carbon-enriched region with an average carbon content of 2.8±0.02at% and an Si average content of 3.4±0.02 at% (Table 3).

Table 3. Chemical composition of phases in the DP steel after intercritical annealing, at%.

	C	**Si**	**Mn**
Ferrite	0.06±0.003	2.3±0.02	0.97±0.01
Martensite	2.8±0.2	3.4±0.02	1±0.01

Since the microstructure of DP steel predominantly consists of ferrite and martensite, it was assumed that the carbon-enriched region represents martensite, while the carbon-depleted region represents ferrite. The levels of Si and Mn were higher in martensite than in ferrite (Table 3). Since the retained austenite and bainite volume fraction in the DP steel was relatively low, they were not detected using APT technique.

The TRIP steel has a more complex microstructure with the presence of ferrite, retained austenite, bainite and martensite. However, the APT analysis was concentrated on the study of retained austenite and ferrite as the main phases. Based on the phase compositional analysis obtained from APT data and calculation using the number of atoms, it appeared that the average carbon content of

retained austenite was 5.2±0.01at%, which is close to the carbon content estimated using X-ray, while the average carbon content of ferrite was 0.02±0.01at% (Table 4). The APT also showed the homogeneous distribution of Mn and Si within the retained austenite and its higher contents in retained austenite than in polygonal ferrite (Table 4). The carbon content of ferrite in the TRIP steel was lower than in the DP steel.

Table 4. Chemical composition of phases in the TRIP steel after intercritical annealing, at%.

	C	**Si**	**Mn**
Ferrite	0.02±0.01	3.9±0.04	0.9±0.03
Austenite	5.2±0.01	4.4±0.05	1.2±0.03

The several atom maps of the DP samples after bake-hardening at 175°C for 30 min showed the carbon-enriched region around the dislocations in the polygonal ferrite (Figs. 4a). The concentration profiles across the dislocations showed an increase in average carbon content around the dislocation to 0.1±0.05at% with maximum level of 0.8±0.02at% (Fig. 4c), while the concentration of Si and Mn did not vary.

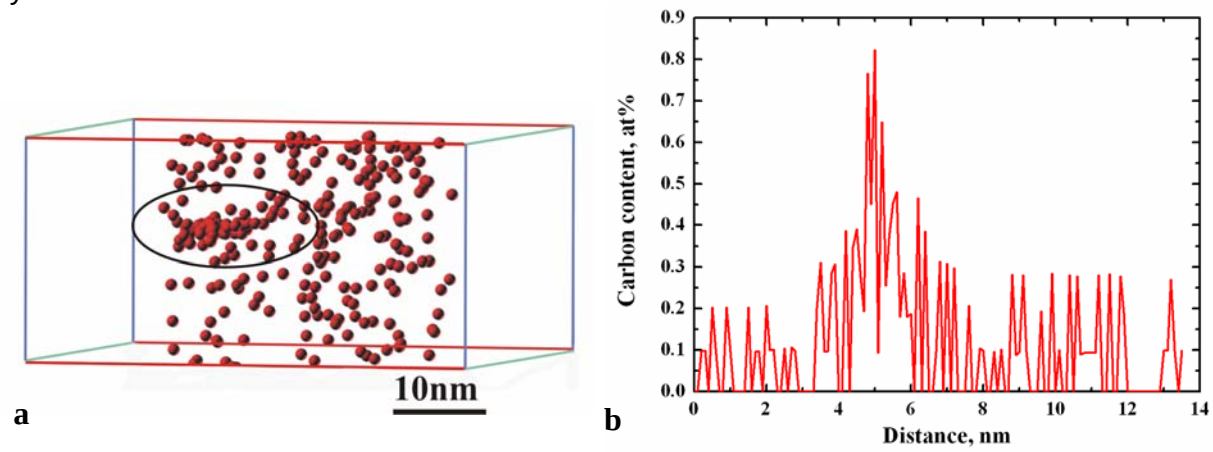

Fig. 4. Representative atom map of carbon segregation around dislocation (a) and corresponding carbon concentration profile across the dislocation line (b). Analysed volume contains 6318154 atoms.

APT confirmed the decomposition of martensite with formation of Fe carbides, which was observed by TEM (Figs. 5a, b). The compositional analysis revealed that the average composition of carbides is 21±2at% of carbon, 2.6±0.01at% of Si and 1.3±0.01at% of Mn.

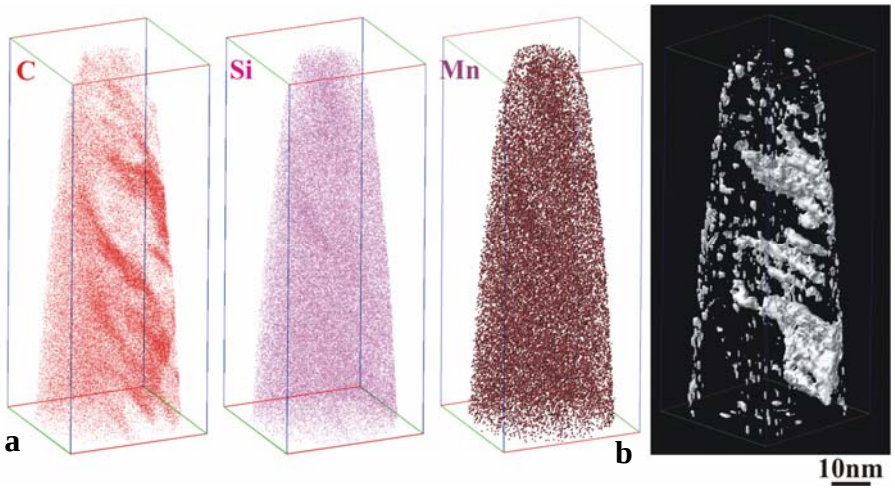

Fig. 5. APT characterisation of martensite in the DP steel after bake-hardening treatment: (a) C, Si, Mn atom maps, (b) 6at% C iso-concentration surfaces. Analysed volume contains 3354460 atoms.

The compositional analysis of polygonal ferrite in the TRIP steel after bake-hardening did not reveal any compositional changes. However, some of the retained austenite crystals showed the segregation of carbon along the dislocations with an average increase in the carbon content from ~ 5.2at% to 5.8at % , while the distribution of Si and Mn remained constant (Fig. 6).

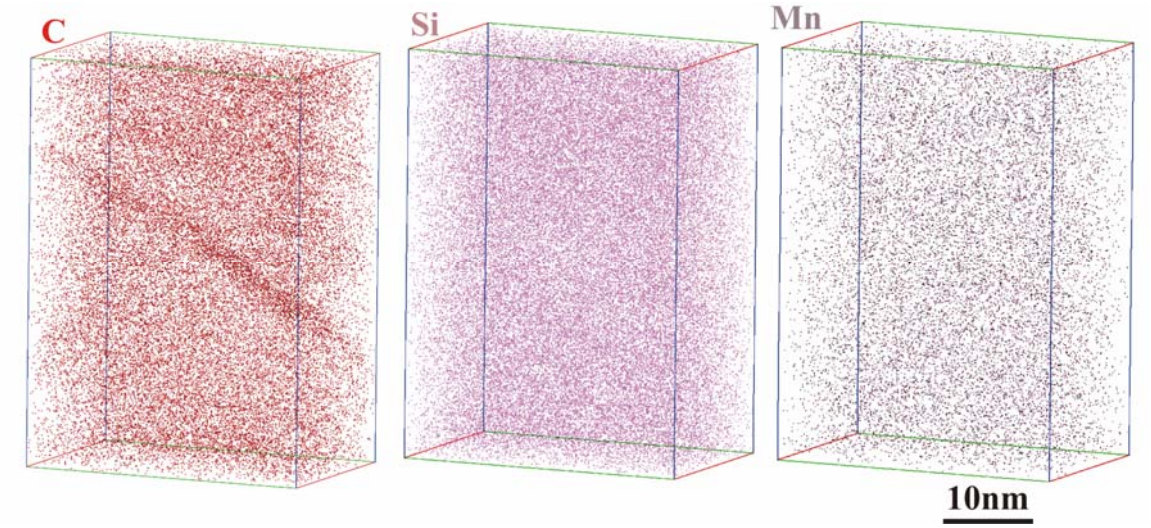

Fig. 6. C, Si and Mn atom map of retained austenite in the TRIP steel after bake-hardening treatment. Analysed volume contains 8727188 atoms.

Discussion

The increase in yield strength (~ 150MPa) after a single bake-hardening treatment and the appearance of the upper yield point was only observed in the DP steel. Moreover, only the DP steel displayed a local minima in the work hardening rate (Fig. 1c). The presence of the upper yield point in the bake-hardened DP steel is evidence of dislocation pinning in the ferrite during the baking treatment. Furthermore, the strain-hardening rate behavior of the DP steel appears to be sensitive to the pinning of the mobile dislocations in the ferrite matrix.[11, 16] Hence, the transition from a continuous behavior of the strain-hardening rate curve of DP steel after processing to the discontinuous behavior after BH could be due to the formation of Cottrell atmospheres that pin the mobile dislocations in the ferrite.[11] However, the average dislocation density of ferrite in the DP steel is lower than in the TRIP steel, so a more pronounced BH effect would be expected in the TRIP steel if the same carbon content exists in the ferrite. However, APT showed that the carbon content of ferrite in the DP steel was significantly higher than in the TRIP steel in spite of higher number of Fe_3C carbides in the DP steel due to the lower Si content than in the composition of TRIP steel. This is probably due to the difference in the temperatures of polygonal ferrite formation in these two steels and the formation of high temperature TiC carbides in the TRIP steel. Moreover, the formation of a high volume fraction of ‘as-quenched” martensite in a soft polygonal ferrite matrix of the DP steel during quenching led to the formation of the plastic deformation zones with a much higher local dislocation density (Table 2) in the ferrite matrix surrounding the martensite than in the rest of the ferrite matrix. Based on the APT study, it appeared that the carbon can segregate to dislocations during bake-hardening in the DP, which is due to the high carbon content of the ferrite. Moreover, since an increase in dislocation density was observed at the martensite/ferrite interface, the carbon may partition from martensite to surrounding ferrite with high dislocation density during treatment due to the supersaturation of martensite with carbon. In this case, it is possible for solute carbon to lock dislocations in these local regions leading to the appearance of the upper yield point. The enrichment of ferrite in Si as Si is ferrite stabilizer correlates well with the recent finding [17].

For the DP steel there was a permanent increase in ultimate tensile strength. It is suggested that this could be due to the additional formation of fine Fe_3C particles in the ferrite as observed by TEM and in martensite as observed by APT after BH.

For the TRIP steel, the mechanical properties after BH were similar to the as-received (Fig. 1b). The strain-hardening rate and exponent curves also showed similar behaviors (Figs. 1d). The X-ray study of the TRIP steel displayed a slight decrease in the volume fraction of retained austenite during BH. However, the retained austenite that remained in the microstructure after BH had a higher carbon content than the average after processing that increases the chemical stability of retained austenite. Moreover, based on APT study, carbon in the retained austenite crystal can segregate along the dislocation and this could also affect the strain-induced transformation of retained austenite.

Conclusions

The microstructure-property relationship in TRIP and DP steels after intercritical annealing and bake-hardening has been analyzed using TEM and APT. The most important findings from this research have been that:

1. The increase in yield strength of DP steel after bake-hardening was most likely due to the higher carbon content of the ferrite matrix and the formation of the plastic deformation zones in ferrite at martensite/ferrite interface that were saturated with carbon;
2. The BH treatment leads to the formation of Fe_3C carbides in the martensite of the DP steel and the retained austenite crystal defects can be saturated with carbon during bake-hardening of the TRIP steel.

References

1. Y. Sakuma, O. Matsumura and H. Takechi: Metall. Trans. A, 22A(1991), 489.
2. V.F. Zackay, E.R. Parker, D. Fahr and R. Bush: Transactions of the ASM, 60(1967), 252.
3. A.H. Nakagawa and G. Thomas: *Metall. Trans. A*, 1985, vol. 16, pp. 831-40.
4. O. Matsumura, Y. Sakuma and H. Takechi: *Trans. ISIJ*, 1987, vol. 27, pp. 570-79.
5. M.S. Rashid: *Formable HSLA and Dual-Phase Steels*, 1979, vol. 244, pp. 1-24.
6. O. Matsumura, Y. Sakuma and H. Takechi: *Scripta Metall.*, 1987, vol. 21, pp. 1301-06.
7. G.R. Speich, V.A. Demarest: *Metall. Trans. A*, 1981, vol. 12A, pp. 1419-28.
8. L.J. Baker, S.R. Daniel and J.D. Parker: *Mat. Science and Tech.*, 2002, vol. 18, pp. 355-68.
9. A.H. Cottrell and B.A. Bilby: *Proc. Phys. Soc.*, 1949, vol. A62, pp. 49-62.
10. T. Senuma: *ISIJ Int.*, 2001, vol. 41, No 6, pp. 520-32.
11. T. Waterschoot, A.K. De, S. Vandeputte and B.C. De Cooman: Metall. Trans*. A*, 2003, vol. 34, pp. 781-91.
12. I.B. Timokhina, P.D. Hodgson and E.V. Pereloma: Metall. Trans*. A*, 2007, vol. 38, pp. 2442-2454.
13. P.B. Hirsch, R.B. Nicholson, A. Howie, D.W. Pashley and M.J. Whelan: *Electron Microscopy of Thin Crystals*, Butterworths, London, 1965, pp. 51-4.
14. B.D. Cullity: “Elements of X-Ray Diffraction”, Addison-Wesley Publishing Company, Inc., London, England, 1978, pp. 411-415.
15. M.K. Miller, *Atom Probe Tomography*, New York (NY), Kluwer Academic/Plenum Press, 2000.
16. T. Huper, S. Endo, N. Ishikawa and K. Osawa: *ISIJ Int*., 1999, vol. 39, No.3, pp. 288-94.
17. E.V. Pereloma, I.B. Timokhina, M.K. Miller, P.D. Hodgson, Acta Materaila, vol. 55, 2007, pp. 2587-2598.